

# Permeability of Acetic Acid through Organic Films at the Air–Aqueous Interface

Jessica B. Gilman and Veronica Vaida\*

Department of Chemistry and Biochemistry and CIRES, University of Colorado, Campus Box 215, Boulder, Colorado 80309-0215

Received: February 26, 2006; In Final Form: April 28, 2006

Recent field studies of collected aerosol particles, both marine and continental, show that the outermost layers contain long-chain ( $C \geq 18$ ) organics. The presence of these long-chain organics could impede the transport of gases and other volatile species across the interface. This could effect the particle's composition, lifetime, and heterogeneous chemistry. In this study, the uptake rate of acetic acid vapor across a clean interface and through films of long-chain organics into an aqueous subphase solution containing an acid–base indicator (bromocresol green) was measured under ambient conditions using visible absorption spectroscopy. Acetic acid is a volatile organic compound (VOC) and is an atmospherically relevant organic acid. The uptake of acetic acid through single-component organic films of 1-octadecanol ( $C_{18}H_{38}O$ ), 1-triacontanol ( $C_{30}H_{62}O$ ), *cis*-9-octadecen-1-ol ( $C_{18}H_{36}O$ ), and nonacosane ( $C_{29}H_{60}$ ) in addition to two mixed films containing equimolar 1-triacontanol/nonacosane and equimolar 1-triacontanol/*cis*-9-octadecen-1-ol was determined. These species represent long-chain organic compounds that reside at the air–aqueous interface of atmospheric aerosols. The *cis*-9-octadecen-1-ol film had little effect on the net uptake rate of acetic acid vapor into solution; however, the uptake rate was reduced by almost one-half by an interfacial film of 1-triacontanol. The measured uptake rates were used to calculate the permeability of acetic acid through the various films which ranged from  $1.5 \times 10^{-3} \text{ cm s}^{-1}$  for 1-triacontanol, the least permeable film, to  $2.5 \times 10^{-2} \text{ cm s}^{-1}$  for *cis*-9-octadecen-1-ol, the most permeable film. Both mixed films had permeabilities that were between that of the single-component films comprising the mixture. This shows that the permeability of a mixed film may not be solely determined by the most permeable species in the mixture. The permeabilities of all the films studied here are discussed in relation to their molecular properties, pressure–area isotherms, and atmospheric implications.

## Introduction

It has been well documented that organics comprise a significant portion of the composition of atmospheric aerosols.<sup>1–8</sup> These organics can be water-soluble<sup>9,10</sup> and reside in the bulk of an aqueous aerosol, or they can partition to the interface if they are water insoluble.<sup>11–13</sup> Surface-sensitive analysis techniques, such as time-of-flight secondary ion mass spectrometry (TOF–SIMS), have revealed that the outermost layers of both marine and continental aerosols contain long-chain organics leading to the formation of an organic coating.<sup>14–16</sup> The properties of an atmospheric aerosol may ultimately be determined by the organic layer at the surface of the particle.<sup>17–19</sup> The presence of an organic film on atmospheric aerosols could impede the transport of gases and other volatile species across the interface, including the uptake of water, allowing the particle to grow in humid environments, and the evaporation of water contained in the core of the aerosol.<sup>20</sup> The transport of other volatile species, such as acetic acid and other small organics, across the interface of aerosols could have a direct effect on a particle's composition, lifetime, and heterogeneous chemistry.

The change in condensation/evaporation rates of gaseous species across the air–water interface when an organic film is present is attributed to the added resistance to gas transport from the monolayer.<sup>21</sup> The total resistance to gas transport across the air–water interface with an organic film,  $pA/U_T$ , is simply the

sum of the monolayer resistance,  $r$ , and the bulk resistances,  $pA/U_o$ , as shown:<sup>22,23</sup>

$$\frac{pA}{U_T} = \frac{pA}{U_o} + r \quad (\text{E1})$$

where  $p$  is the pressure of the permeating gas ( $\text{cm}^3 \text{ cm}^{-3}$ ) and  $A$  is the surface area of the interface ( $\text{cm}^2$ ). The total resistance of the transport pathway can be determined by measuring the uptake rate ( $\text{cm}^3 \text{ s}^{-1}$ ) of a gas across a clean interface,  $U_o$ , and the uptake rate when a film is present,  $U_T$ . The difference between these two pathways is equal to the resistance  $r$  of the film ( $\text{s cm}^{-1}$ ), which is a property of the film itself rather than of the system and is independent of the method of measurement and the conditions of the experiment (i.e., the absolute values for  $p$  and  $A$ ).<sup>20</sup> The permeability  $P_f$  ( $\text{cm s}^{-1}$ ) of the film is determined by simply taking the reciprocal of the resistance ( $1/r$ ).<sup>23</sup>

The resistances and permeabilities of various organic films as a function of their composition and structure have been studied by systematically varying the length of the hydrocarbon chain,<sup>24,25</sup> the functionality of the polar headgroup,<sup>26–28</sup> and the structure of the hydrocarbon chain.<sup>23,29</sup> For a homologous series of compounds, further lengthening the hydrocarbon chain has been determined to reduce the permeability of gaseous species across the air–aqueous interface.<sup>23–26,29</sup> Our study expands on this observation by measuring the permeability of acetic acid through a  $C_{30}$  linear alcohol (1-triacontanol) in comparison to a  $C_{18}$  alcohol (1-octadecanol). The permeability of another film-

\* Corresponding author. Fax: +1-303-492-5894. E-mail address: Vaida@colorado.edu.

forming compound that has not been previously studied is a C<sub>29</sub> linear alkane (nonacosane). This alkane is not expected to self-assemble because its lack of a polar headgroup, but it has been shown to be extremely stable at the air–water interface over long periods of time<sup>30</sup> and could affect the transport rate across the interface. Compounds that are not capable of forming highly ordered films upon compression, such as branched-chain surfactants, have little effect on the permeability rate.<sup>31–33</sup> This was studied here by comparing the permeability of a C<sub>18</sub> bent-chain alcohol (*cis*-9-octadecen-1-ol) to its straight-chain counterpart (1-octadecanol).

The composition of atmospheric aerosols is highly complex and pure films of surfactants are not expected to occur in nature. The effect of the homogeneity (i.e., miscibility or immiscibility) of a mixed film on the permeability of acetic acid was investigated. Miscible films are considered to be more homogeneously mixed than immiscible films, which consist of domains of the pure components. Barnes and co-workers proposed that water evaporation only occurs through interdomains, regions between the pure domains, because the pure domains will be highly ordered and impermeable to the water molecules.<sup>20,34</sup> Thus, it could be expected that immiscible films are more permeable than miscible films because of the inhomogeneities in the film's structure.

The permeability of a volatile species is expected to be dependent upon its molecular dimensions and interactions with both the organic film and the subphase. Acetic acid represents a prototypical volatile organic compound (VOC) and is one of the most abundant organic acids in the atmosphere.<sup>35</sup> Its absorption on water<sup>36,37</sup> and organic surfaces<sup>38,39</sup> has previously been investigated, but to the authors' knowledge this is the first report of the uptake of acetic acid through organic films on an aqueous subphase. Acetic acid is a relatively large compound compared to water or CO<sub>2</sub>, whose permeabilities have been previously studied. Larger volatiles will diffuse more slowly, and there must be an area in the film large enough for the permeating species to fit through, which results in both a decreased uptake rate and permeability.<sup>20,21</sup> The ability of acetic acid to change the pH of the subphase will give valuable insight as to how the pH of an aerosol's core may change as a function of its composition as it ages in the atmosphere.

In this study, the uptake of acetic acid through single-component and mixed organic films at the air–aqueous interface was measured by visible absorption spectroscopy. The organic film components studied here were chosen to represent species commonly found on atmospheric particles and to extend the experimental database with atmospherically relevant chemical systems. All of the film components are long-chain organics (C ≥ 18), water insoluble, and will partition to the air–water interface. The resistances and permeabilities of these films were determined by comparing the uptake rate of acetic acid with and without a film present at the air–water interface. The permeabilities of these films are discussed in relation to their molecular properties, pressure–area isotherms, and their atmospheric implications.

## Experimental Section

**Materials.** All materials were purchased from Aldrich Chemical Co., Inc. (Milwaukee, WI) and used without further purification. The aqueous subphase was composed of a 1:40 dilution of bromocresol green indicator (0.04 wt % solution in water, Aldrich) in HPLC water (Burdick and Jackson, Muskegon, MI). Individual solutions of the following were made in benzene: 1-octadecanol (C<sub>18</sub>H<sub>38</sub>O, 99%), *cis*-9-octadecen-1-ol

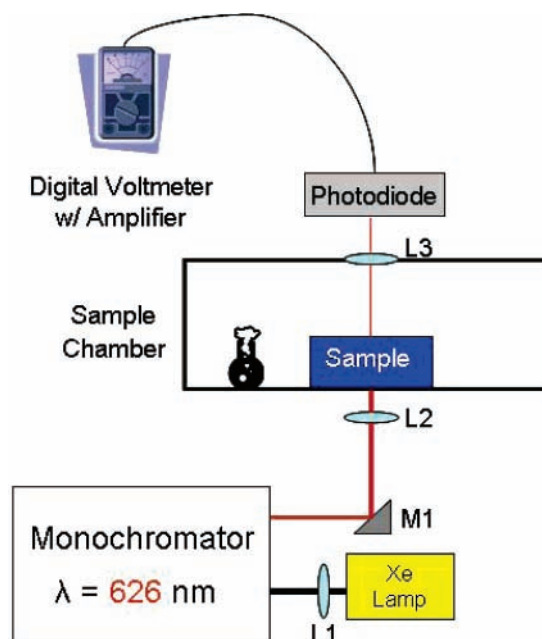


**Figure 1.** Schematic diagram of the experimental setup.

(C<sub>18</sub>H<sub>36</sub>O, 99%), 1-triacontanol (C<sub>30</sub>H<sub>62</sub>O, 99%), and nonacosane (C<sub>29</sub>H<sub>60</sub>, 99%). Two binary solutions were composed of equimolar 1-triacontanol/nonacosane and 1-triacontanol/*cis*-9-octadecen-1-ol in benzene. Gas-phase acetic acid was generated inside the sample chamber from the vapor pressure above 1.0 mL of a 40 vol % solution of glacial acetic acid (Mallinckrodt Chemicals) in water. To avoid temperature fluctuations, the vial containing the acetic acid solution remained in a thermally insulating mineral oil bath at room temperature.

**Sample Preparation.** A volumetric pipet was used to transfer 10 mL of the indicator solution into a quartz dish with an optically flat bottom. The mass of the indicator solution was also measured to ensure an exact amount of subphase volume, and thus the same optical path length through the sample. The sample dish was placed inside the sample chamber prior to the addition of the film. The organic films were formed by dropwise addition of the single-component or binary spreading solutions to the surface of the aqueous subphase. The spreading solvent benzene was allowed to evaporate for a minimum of 30 min.

All films contained a total of  $7.14 \times 10^{16}$  molecules and occupied a surface area of 16.97 cm<sup>2</sup> as determined by the dimensions of the dish. The thin films studied here were naturally formed and represent less-organized films that are more applicable to the environment. For reproducibility in the organic films' structure, all films studied here were at their equilibrium spreading pressure (on average approximately 20 mN m<sup>-1</sup>). For these films, monolayer coverage was exceeded resulting in the formation of a few minute islands of crystalline material at the interface which are thicker than a single monolayer. For the vast majority of the interfacial surface area, excluding the islands, the organic film is approximately a monolayer thick. Several trials were averaged so that any differences in each of the individual films would not contribute to the overall measurement.

**Instrumentation and Procedure.** A schematic diagram of the experimental setup is shown in Figure 1. Light from a 50 W Xe lamp (Hamamatsu) was focused on the entrance slit of a monochromator (Jobin Yvon HRS-2) set at 626 nm corresponding to the maximum absorbance of the dark blue indicator solution. The light exiting the monochromator was directed upward by a 45° mirror through a lens (L1) and through an

opening in the bottom of the sample chamber. The steel sample chamber (33 × 20 × 9.5 cm) has a removable face plate with gas inlets and two openings (4.0 cm diameter) on the top and bottom of the chamber. The quartz dish containing the sample is placed directly over the opening in the bottom of the sample chamber so that the light is absorbed as it passes longitudinally through the sample solution, where it is then focused (L2) on the photodiode detector, amplified, and recorded by a digital voltmeter (Fluke Corp., USA). The voltmeter measured the DC signal at 0.1 Hz and recorded the average of 20 s intervals.

The walls of the sample chamber were washed with a dilute solution of sodium bicarbonate, rinsed with water, and purged with N<sub>2</sub> between each trial. This ensured that no acetic acid vapor remained in the chamber or on the walls. Experiments were conducted on samples that had no film added (a clean interface) and those with single-component and mixed films. The signal for all samples was monitored for at least 10 min in order to ensure that it remained constant and that there was no residual acetic acid in the chamber. Recording of the time sequence was started when the open vial containing acetic acid was inserted into the sample chamber which was then securely closed. Both the sample dish and the acetic acid vial were placed in the same positions inside the chamber ensuring that the distance the acetic acid vapor has to diffuse is held constant. All trials were performed at room temperature.

The intensity (*I*) of light reaching the detector was monitored as a function of the sample's exposure time to acetic acid vapor. The intensity of the reference solution (*I*<sub>0</sub>) containing 10 mL HPLC water in the same quartz dish was collected prior to every experiment. As the amount of acetic acid permeating the interface and diffusing into the subphase solution increases, the pH decreases changing the indicator solution from blue (neutral, low transmission) to yellow (acidic, high transmission). As the acetic acid concentration in solution increases, the percent transmission %*T* = (*I*/*I*<sub>0</sub>) × 100% increases. The relatively slow diffusion of acetic acid in the indicator solution resulted in slight color gradients within the subphase. To compensate for this effect, the incident light was kept diffuse with a large spot size of ~10 cm<sup>2</sup> so that the transmission was averaged over a large area. A minimum of three reproducible transmission curves were acquired for each film studied.

The amount of acetic acid dissolved in the subphase solution was determined from a working curve obtained by measuring the percent transmission of known concentrations of acetic acid in the indicator solution. The concentration of acetic acid in solution (mol L<sup>-1</sup>) was used to determine the volume (cm<sup>3</sup>) of acetic acid vapor adsorbed by the sample as a function of time.

**Pressure–Area Isotherms.** A PTFE Langmuir trough (52 × 7 × 0.5 cm) with two mechanical PTFE barriers was used to collect surface pressure–area isotherms of all the films studied here on both water and indicator solution subphases. The software and computer interface used for operation were purchased from NIMA (NIMA Technology Ltd., U.K.). Surface pressures were measured with a Wilhelmy plate of chromatography paper (Whatman Chr 1) suspended from a balance as a function of surface area. Organic monolayers were formed by dropping the spreading solution evenly over the entire air–aqueous surface area between the barriers. The film-forming compounds spontaneously spread across the interface and the spreading solvent evaporates. Pressure–area isotherms were collected at room temperature using a constant compression rate of 100 cm<sup>2</sup> min<sup>-1</sup>. At least three reproducible isotherms were obtained for each film component.

## Results

Visible absorption spectroscopy was used to directly and continuously measure the uptake of acetic acid vapor into a liquid subphase across a clean interface and through organic films at the air–aqueous interface. The technique is readily employable to measuring the permeability of a number of different acidic or basic gas-phase species through various surface films. Analogous spectroscopy techniques have been developed by others to probe the uptake dynamics and pH of aqueous aerosols<sup>40</sup> and the evaporation kinetics of organically coated aqueous aerosols.<sup>41</sup> The transport of acetic acid vapor into the aqueous subphase involves a number of steps including (1) evaporation, (2) diffusion throughout the sample chamber, (3) permeation of the interface with or without an organic film, (4) solvation in the aqueous subphase, and (5) diffusion throughout the subphase solution. It was assumed that these processes were consistent for all trials performed under ambient conditions except for the permeation of the organic film, the composition of which was the only variable. The uptake measurements reported here are for the net rate of acetic acid uptake, which is defined as the difference in the absolute rates of evaporation and condensation of acetic acid over the time scale of this experiment. All the films were naturally formed and are at their equilibrium spreading pressures, so the effect of the surface pressure on the uptake rates will not be detailed.

The film-forming compounds studied here included two straight-chain alcohols, a bent-chain alcohol, and a straight-chain alkane. From this point on, 1-octadecanol (C<sub>18</sub>H<sub>38</sub>O), 1-triacontanol (C<sub>30</sub>H<sub>62</sub>O), nonacosane (C<sub>29</sub>H<sub>60</sub>), and *cis*-9-octadecen-1-ol (C<sub>18</sub>H<sub>36</sub>O) will be abbreviated as C<sub>18</sub>OH, C<sub>30</sub>OH, C<sub>29</sub>, and *bent*-C<sub>18</sub>OH, respectively. These compounds were chosen to represent the wide range of long-chain organic species that are atmospherically relevant. Additionally, these compounds, unlike carboxylic acids and amines, do not contain ionizable head-groups so they could not contribute to changes in the pH of the subphase and their films would not be altered by the decreasing pH of the subphase as the experiment proceeded. Pressure–area isotherms provided necessary insight into the molecular properties of the film and were used to help explain the differences in permeability for the various films as a function of their structures.

**Acetic Acid Uptake.** The acetic acid uptake through single-component and mixed organic films at the air–aqueous interface is shown in Figure 2, which includes data points from the average of at least three trials and fitted curves to help guide the eye. Error bars were not included in Figure 2 for the sake of clarity. The error in the volume of acetic acid absorbed, which is one standard deviation of the average of at least three trials, increased from ~10% at the start of the experiment to up to 20% at 15 min. This is considered quite reasonable given the sensitivity of the instrument and dynamics of the system. At the start of each trial, the concentration of acetic acid vapor in the sample chamber is zero. This results in a shallow slope for the first minute of the experiment while the acetic acid vapor pressure is increasing. All films were permeable to acetic acid vapor as evidenced by the continuous rise of the traces; however, the uptake rate and permeability of the films was directly dependent on the composition of the film.

As seen in Figure 2, the acetic acid uptake for the *bent*-C<sub>18</sub>-OH is the same as that of a clean interface. The C<sub>29</sub> film results in a significant decrease in the acetic acid uptake compared to that of the clean interface. The uptake of acetic acid through the C<sub>18</sub>OH film is even slower and continues to decrease as the carbon-chain length increases, as seen for the C<sub>30</sub>OH film. Of

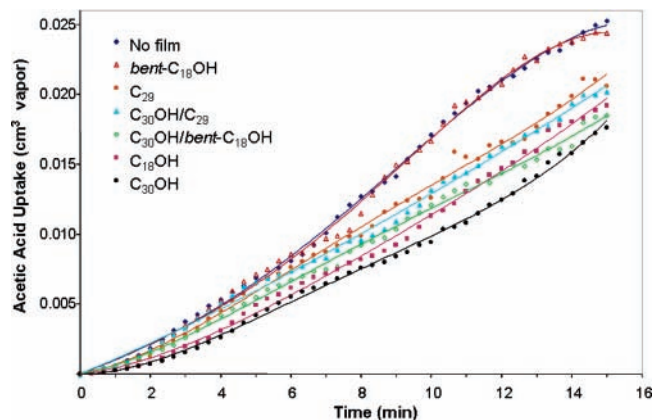


**Figure 2.** Acetic acid uptake when no film is present and for single-component and mixed films at the air–aqueous interface. The y-axis is the volume of acetic acid ( $\text{cm}^3$  vapor) that permeated the interface and dissolved in the bulk subphase. The data points are the average of at least three trials. The solid lines are to help guide to the eye. The films all contained the same number of molecules and all experiments conducted under ambient conditions.

all the films studied here, the  $\text{C}_{30}\text{OH}$  film results in the largest decrease in acetic acid uptake and is thus the least permeable. The uptake through the mixed films is at an intermediate value between both single-component films, so that the uptake of the mixed film is not solely determined by only one of the film components.

To determine the permeability of the films, the linear slope of the uptake plot starting at 5 min and ending at 10 min was determined for all trials. Over this time range the acetic acid vapor-phase concentration is assumed to have approached a steady value estimated from its Henry's law coefficient,  $5500 \pm 290 \text{ M atm}^{-1}$ ,<sup>42</sup> to be  $1.3 \times 10^{-3} \text{ atm}$  (0.97 Torr). The measured uptake rates were used to calculate the film's resistance using (E2). The permeability of a film was calculated by taking the inverse of the resistance. As detailed in Table 1, the  $\text{C}_{30}\text{OH}$  is the least permeable followed by the  $\text{C}_{18}\text{OH}$ , the  $\text{C}_{29}$ , and finally the  $\text{bent-C}_{18}\text{OH}$  which is the most permeable. The error in the uptake rates was determined from a least-squares linear regression. The large source of error in the values for both the monolayer resistances and permeability calculations is a direct result of the large uncertainty in the Henry's law coefficient required to determine the acetic acid gas-phase concentration. Because the gas-phase concentration of acetic acid was not experimentally determined, we present the resistances to permeability and evaporation as approximations.

**Pressure—Area Isotherms.** Isotherms reveal the packing ability of the organic films and are used to confirm the miscibility of the mixed film components. The surface pressure–area isotherms for all of the organic films on a water subphase are shown in Figure 3. There were no appreciable differences in the isotherms for the compounds on a water subphase and the indicator solution subphase. While the indicator is a

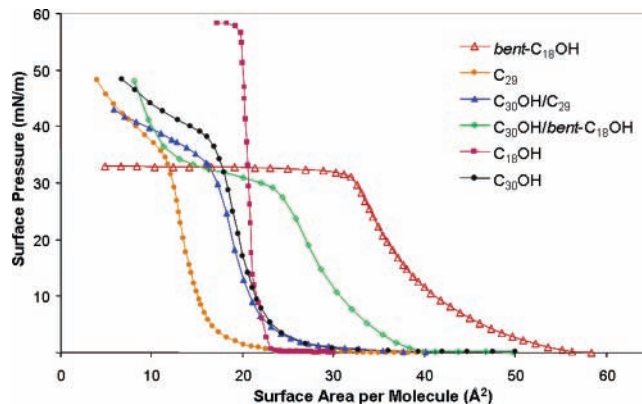


**Figure 3.** Isotherms of the single-component and mixed organic films on water. The mixtures  $\text{C}_{30}\text{OH}/\text{C}_{29}$  and  $\text{C}_{30}\text{OH}/\text{bent-C}_{18}\text{OH}$  are equimolar solutions.

relatively large organic molecule itself, it is highly soluble in water and did not alter the properties of the film for any of the compounds studied here. The isotherms depict the increasing intermolecular interactions between the molecules as the monolayer film is mechanically compressed. The films for the permeability studies were naturally formed, rather than mechanically compressed, and exist at their equilibrium spreading pressures (ESP). Each component has a different ESP, but for simple comparison purposes this can be estimated to be  $\sim 20 \text{ mN m}^{-1}$  on average. Comparing the surface area per molecule for each film at  $20 \text{ mN m}^{-1}$  in the isotherms will provide a general guide to the relative packing of the different films in the permeability studies.

For the single-component films,  $\text{bent-C}_{18}\text{OH}$  remains more expanded compared to its straight-chain counterpart  $\text{C}_{18}\text{OH}$ . The unsaturated bond at the midpoint of the hydrocarbon tail causes a kink in the chain which does not allow  $\text{bent-C}_{18}\text{OH}$  to pack as tightly. The shape of  $\text{C}_{30}\text{OH}$ 's isotherm differs slightly from that of  $\text{C}_{18}\text{OH}$  because of the increased intermolecular forces in its lengthened hydrocarbon tail. The  $\text{C}_{30}\text{OH}$  and the  $\text{C}_{29}$  isotherms are similar in shape; however, the  $\text{C}_{30}\text{OH}$  film is shifted toward a larger surface area as a direct result of the presence of the alcohol headgroup. As illustrated in Figure 3, both the hydrocarbon chain length and the functionality of the polar group affects molecular packing and thus the degree of molecular interactions between film components.

The isotherms of the binary mixtures can be used to determine the miscibility or immiscibility of the film components. The surface area of an immiscible film can be predicted by the additivity rule

$$A_{12} = N_1A_1 + N_2A_2 \quad (\text{E2})$$

where  $A_{12}$  is the average molecular area of the mixed film,  $N_1$  and  $N_2$  are the molar fractions of the components, and  $A_1$  and  $A_2$  are the molecular areas of the two single component films

**TABLE 1: Measured Acetic Acid Uptake Rates and the Calculated Monolayer Resistances and Permeabilities of All the Films Studied**

| film composition                             | carbon no./identifier                                | acetic acid uptake rate, $10^5 \text{ cm}^3 \text{ s}^{-1}$ | monolayer resistance, $\text{s cm}^{-1}$ | permeability, $10^3 \text{ cm s}^{-1}$ |
|----------------------------------------------|------------------------------------------------------|-------------------------------------------------------------|------------------------------------------|----------------------------------------|
| no film                                      |                                                      | $3.53 \pm 0.18$                                             |                                          |                                        |
| 1-triacontanol                               | $\text{C}_{30}\text{OH}$                             | $1.69 \pm 0.08$                                             | $670 \pm 100$                            | $1.5 \pm 0.2$                          |
| 1-octadecanol                                | $\text{C}_{18}\text{OH}$                             | $1.92 \pm 0.10$                                             | $510 \pm 90$                             | $2.0 \pm 0.4$                          |
| nonacosane                                   | $\text{C}_{29}$                                      | $2.22 \pm 0.11$                                             | $360 \pm 80$                             | $2.8 \pm 0.7$                          |
| <i>cis</i> -9-octadecen-1-ol                 | $\text{bent-C}_{18}\text{OH}$                        | $3.31 \pm 0.17$                                             | $40 \pm 60$                              | $25 \pm 42$                            |
| 1-triacontanol/nonacosane                    | $\text{C}_{30}\text{OH}/\text{C}_{29}$               | $1.98 \pm 0.10$                                             | $480 \pm 90$                             | $2.1 \pm 0.4$                          |
| 1-triacontanol/ <i>cis</i> -9-octadecen-1-ol | $\text{C}_{30}\text{OH}/\text{bent-C}_{18}\text{OH}$ | $2.15 \pm 0.11$                                             | $390 \pm 90$                             | $2.5 \pm 0.5$                          |

at the same pressure.<sup>43</sup> An immiscible film, or one that is phase separate, will abide by this rule as is the case for the  $C_{30}OH/bent-C_{18}OH$  film where  $A_{12} = 27.7 \text{ \AA}^2$  and the measured area of the mixed film is  $27.5 \text{ \AA}^2$  at  $20 \text{ mN m}^{-1}$ . The immiscibility of this mixed film is a direct result of the large differences in both the hydrocarbon chain length and compressibilities related to their differing linearity.

A miscible film deviates from the additivity rule, indicating that there are molecular interactions between the film components. For the  $C_{30}OH/C_{29}$  film,  $A_{12} = 16.3 \text{ \AA}^2$  and the measured area of the mixed film is much larger at  $18.5 \text{ \AA}^2$  at  $20 \text{ mN m}^{-1}$ . The presence of the nonpolar alkane within the close-packed film of  $C_{30}OH$  increases the area per molecule of the mixed film leading to a slight expansion of the more homogeneous mixed film compared to the separate domains of each film component in an immiscible film.<sup>44</sup>

## Discussion

The films studied here are laboratory representations of organic films on aqueous aerosols. While there are expected to be subtle differences between the permeability of films on planar surfaces and those on droplets, several uptake<sup>31,45</sup> and evaporation<sup>46,47</sup> studies conducted on droplets show similar effects related to the organic film. These results support the use of planar Langmuir films as simplified proxies for organic films on aqueous aerosols. The structure and properties of an organically coated aerosol have been qualitatively defined in an attempt to clarify the wide-ranging effects that an organic film may have on an aerosol's properties.<sup>17,18,48–51</sup> The organic film is expected to act as a semipermeable membrane that is reactive toward atmospheric radicals.<sup>17,52</sup> Thus, the organic film itself is dynamic and its physical, chemical, and morphological properties as well as that of the aerosol itself will change according to its environment and its age in the atmosphere. The dynamic nature of the film's properties would have a direct effect on the aerosol's ability to absorb or scatter radiation and its ability to absorb water and act as cloud condensation nuclei. Heterogeneous chemical reactions could also be impeded and the chemical composition of the particle in the atmosphere as it ages could be altered. This publication is focused on revealing the effects that long-chain organic films have on the transport of acetic acid, a prototypical gas-phase organic in the atmosphere, across the air–aqueous interface.

**Single-Component Films.** All films, except for the *bent*- $C_{18}OH$ , reduced the uptake rate of acetic acid into the subphase solution. The degree to which the uptake rate was reduced depended upon the architecture of the film, as determined by its composition and illustrated by the pressure–area isotherms. Our data closely follows the general trends for evaporation of water through films as a function of their architecture. For the homologous pair  $C_{18}OH$  and  $C_{30}OH$ , the uptake rate was considerably less for the longer-chain alcohol. This is in excellent agreement with the work of La Mer and co-workers who studied a series of alcohols from  $C_{14}$  up to  $C_{22}$ <sup>25</sup> as well as  $C_{17}$  to  $C_{20}$  fatty acids<sup>24</sup> and showed that the permeabilities of these films are inversely related to the carbon-chain length.

The actual effect of a film on the evaporation rate at the interface can be quantified by calculating the ratio  $r_0/r$ , where  $r_0$  is the resistance of a clean water interface and  $r$  is the resistance when a film is present.<sup>24</sup> The value of  $r_0$  for acetic acid is not reported here, but can be approximated from literature sources and is analogous to the fraction of acetic acid molecules in solution that have enough energy to desorb from the indicator

subphase into the gas-phase. The mass accommodation coefficient,  $\alpha$ , for acetic acid on a clean water interface at 273 K is reported to be 0.067.<sup>37</sup> This value can be used to approximate the resistance of evaporation of acetic acid at the interface when no film is present by using the equation  $r = 4/(\alpha\langle v \rangle)$ , where  $r$  is resistance to evaporation ( $\text{s cm}^{-1}$ ),  $\alpha$  is the mass accommodation coefficient, and  $\langle v \rangle$  is the mean thermal velocity of the gas ( $\text{cm s}^{-1}$ ).<sup>53</sup> The resistance to evaporation of acetic acid from solution with a clean water interface is thus approximated to be  $1.9 \times 10^{-3} \text{ cm s}^{-1}$  at 273 K. This is in close agreement with the resistance to water evaporation from a clean interface,  $1.9 \times 10^{-3} \text{ cm s}^{-1}$  at 298 K.<sup>24</sup> Assuming  $r_0 = 1.9 \times 10^{-3} \text{ cm s}^{-1}$ , the alcohol and alkane films studied here reduce the rate of evaporation of acetic acid by a factor of  $\sim 10^6$ . Archer and La Mer<sup>24</sup> report a decrease in the evaporation rate of water through fatty acid films of similar carbon number to be  $\sim 10^4$ . This difference in evaporation rates is not unexpected and is the result of two main factors: (1) fatty acid films have been found to have lower resistances to evaporation because they do not pack as tightly as fatty alcohol films<sup>23,54,55</sup> and (2) the permeants, acetic acid and water, have different molecular dimensions.

By studying the permeation of various gases through the same film, one can start to isolate the molecular properties of the permeant and their effects on uptake rates and permeabilities. Blank<sup>26</sup> reports the permeability of  $CO_2$ ,  $O_2$ ,  $N_2O$ , and  $H_2O$  through  $C_{18}OH$  films on an aqueous subphase to be 0.0044, 0.0032, 0.0010, and  $0.30 \text{ cm s}^{-1}$ , respectively. We report here that the permeability of acetic acid through a  $C_{18}OH$  film on an aqueous subphase to be  $0.0020 \text{ cm s}^{-1}$  at room temperature. Thus, water is 150 times more permeable than acetic acid through a  $C_{18}OH$  film while  $CO_2$  and  $O_2$  are only about twice as permeable. These differences can be related to the molecular dimensions of the molecules and the presence of water vapor in the systems. Blank postulates that water vapor, which is intrinsic to these studies where water is the subphase, acts as an additional barrier to the permeation of all other gases.<sup>56</sup> This added barrier to permeation could significantly decrease the mass transport of gases across the interface of aerosols because the atmosphere contains significant amounts of water vapor in addition to other gases that could compete in the permeation process.

The uptake and permeability of volatile species are dependent upon its molecular dimensions as well as its interactions with the organic film and/or subphase. Not only will larger volatile species diffuse more slowly resulting in a decreased uptake rate, but there must be an area in the film large enough for a permeating species to fit through.<sup>20,21,56</sup> If the volatile species experiences intermolecular interactions, then the uptake of trace gases is likely to occur via the attraction between the trace molecule and the organic film.<sup>38</sup> Films containing shorter-chain organic surfactants ( $C \leq 8$ ) are porous<sup>57</sup> and have been shown to actually enhance the uptake of certain gas-phase species.<sup>58,59</sup> Thus, organics at the interface may be analogous to an “organic solvent”<sup>39</sup> but also provide sites for hydrogen-bonding and protonation,<sup>59</sup> both of which will affect the uptake rate of the individual species. If these interactions are favorable enough, the initial uptake may be enhanced, but the mass transport into the subphase could be reduced as the “permeant” would rather reside at the interface rather than be transported into the bulk. Further lengthening the hydrocarbon chain ( $C \geq 8$ ) will eventually increase the effectiveness of the film as barrier to mass transport resulting in decreased uptake rather than further enhancing it.

The interaction of water vapor and atmospheric aerosols is of great interest as it relates to their lifetime<sup>60–62</sup> and their hygroscopic properties.<sup>63–67</sup> Rubel and Gentry<sup>68</sup> showed that the water accommodation coefficient, the fraction of water molecules accommodated after striking the surface, decreased with increasing surface coverage by a fatty alcohol film. As organic films are transported and age in the atmosphere, they are susceptible to oxidization via heterogeneous reactions with O<sub>3</sub>, •OH, NO<sub>x</sub>, and halide radicals. As the initially hydrophobic organic film is oxidized and becomes more hydrophilic, the uptake rate of water is expected to increase. This is indeed the case, as the amount of water absorbed by an organic film has been shown to be correlated with the oxidation state of the organic film.<sup>69</sup>

The C<sub>29</sub> film studied here represents a completely hydrophobic film. Not as many permeability studies have been done on alkane films presumably because they cannot self-assemble at the air–water interface and are not expected to be efficient barriers to permeation. However, it has become evident that these compounds are particularly important to atmospheric surfaces. Nonacosane (C<sub>29</sub>) has been shown to be long-lived at the air–water interface over atmospherically relevant time scales,<sup>30</sup> and octadecane (C<sub>18</sub>) has been shown to remain at the interface longer when in the presence of a fatty acid.<sup>70</sup> These species could not only affect mass transport across the interface, but also undergo heterogeneous radical reactions further altering the structure and permeability of the film. We have shown here that C<sub>29</sub> films result in a decreased uptake of acetic acid. This agrees with Daeumer<sup>31</sup> who has shown that films of hexadecane (C<sub>16</sub>) greater than 2 nm thick were capable of reducing mass transport of gaseous ammonia across the interface of a sulfuric acid aerosol decreasing the bulk neutralization reaction rate. A typical oxidation product of C<sub>29</sub> with •OH would be a long-chain alcohol analogous to C<sub>30</sub>OH. If this were the case, then the net uptake rate could be reduced by up to 50% upon oxygenation of the alkane.

Unsaturated bonds can reduce the packing efficiency of the molecule leading to highly expanded films. For the *bent*-C<sub>18</sub>-OH studied here, the double bond caused a “kink” in the hydrocarbon chain resulting in a film that was 10 times more permeable to acetic acid than its straight-chain counterpart. The *bent*-C<sub>18</sub>OH film had the least effect on the acetic acid uptake of all the films studied. This is in good agreement with previous work showing that oleic acid, a similarly unsaturated compound, did not affect the uptake rate of water<sup>33</sup> and CO<sub>2</sub>.<sup>23</sup> In the atmosphere, the unsaturated bond is likely to be cleaved upon ozonolysis leading to the formation of smaller, more oxygenated compounds.<sup>71</sup> The presence of these reaction products are expected to alter the film’s properties and have been shown to reduce the evaporation rate of water droplets.<sup>47</sup>

**Mixed Films.** For a mixed film composed of organics with various functionalities and chain-lengths, the film components themselves could act as contaminants reducing the cohesiveness of the film. The interactions between the film molecules and any contaminants are expected to be relatively meager compared to a film of homologous compounds. The contaminants could create permanent holes in the film or at least sites of increased permeability.<sup>24</sup> In these experiments, the molecular properties of the mixed film components were varied in order to determine the effect on uptake and permeability. The mixed film composed of C<sub>30</sub>OH and *bent*-C<sub>18</sub>OH represents an immiscible film composed of two species of differing compressibility which results in minimal interactions between the film molecules. The C<sub>30</sub>OH and C<sub>29</sub> mixture forms a miscible film where the

interactions between the long hydrocarbon chains are maximized. Both films reduced the uptake of acetic acid regardless of their miscibility. The permeabilities of the two mixed films were at intermediate values between that of the single-component films. This observation was also made by Rosano and La Mer<sup>28</sup> as well as Garrett<sup>32</sup> who studied films of binary mixtures. So the presence of *bent*-C<sub>18</sub>OH whose film is highly permeable and could be considered to be a contaminant in the mixed film with C<sub>30</sub>OH, was still effective in reducing the uptake and permeability of acetic acid.

**Subphase Composition.** The pH and salinity of the subphase may significantly alter the architecture of the film and thus have a direct effect on the permeability. In these experiments, the acidity of the subphase increases with time. Fatty alcohols could be ionized if the acidity of the subphase was high enough, much higher than the subphase acidities studied here. For films of ionized alcohols, a marked decrease in the evaporation resistance and the film cohesion has been observed.<sup>72</sup> Langmuir and Schaefer<sup>29</sup> showed that the resistance to evaporation for films of fatty acids increased as the pH decreased. At low pH, the carboxylic acid headgroups remain neutral allowing the surfactants to form highly compact films.

Once a film component, such as fatty acids and alcohols, are ionized by pH changes in the subphase, they can be stabilized by interaction with counterions in the subphase. While the salinity of the subphase was not studied here, it can have two important effects on films at the air–water interface. Gilman et al.<sup>70</sup> showed that fatty acid films on a saline solution can become soluble in the subphase as their salts if the pH is basic. The second effect is termed “salting out.” As the concentration of the salt is increased, the miscibility of the organic with water decreases and the concentration of the organic in the surface layer increases.<sup>73</sup> A nascent marine aerosol is expected to have an aqueous, basic (pH ~ 8), saline core approximating that of the ocean.<sup>17</sup> As the aerosol is transported through the atmosphere it will become more acidic as it is exposed to gases such as CO<sub>2</sub>, SO<sub>2</sub>, and small organic acids. The surface film composition and properties would be continuously changing in accordance with the pH change of the saline core. These observations highlight the dynamic nature of an organic film on an atmospheric aerosol and how its structure, properties, and composition are continuously evolving.

## Conclusions

This study focused on revealing the effect that long-chain organic films have on the transport of acetic acid, an atmospherically relevant gas-phase organic acid, across the air–aqueous interface. We have detailed an experiment that directly measures the acetic acid uptake into a subphase solution with and without an organic film. From the measured uptake rate, we were able to approximate the resistances and permeabilities of the single-component and mixed films. The films studied here were chosen to represent the organic components typically found on atmospheric surfaces, such as at the interface of aerosols. All films were permeable to acetic acid; however, the uptake rates and permeabilities were determined by the composition of the films. Our study expanded on the current data set of film-forming components by measuring the permeability of acetic acid through C<sub>30</sub>OH (1-triacontanol) and a C<sub>29</sub> (nonacosane). Our data closely follow the general trends for evaporation of water through films as a function of their architecture. Long, straight-chain alcohols are the least permeable, while the unsaturated alcohol has little effect on reducing the uptake rate of acetic acid. We were able to compare the

permeability of acetic acid through a C<sub>18</sub>OH (1-octadecanol) film with literature values for the permeability of other volatiles through a similar film elucidating the effect that the molecular properties of the permeant have on its permeability.

The compositions of atmospheric aerosols are known to be highly complex and the presence of single-component films of surfactants is not expected to occur in nature. The effect of mixed films, both miscible and immiscible, on the permeability rate of acetic acids across the aqueous interface was investigated. The miscibility of the film's components was not a significant factor in determining the permeability of the mixed films, both of which proved to be effective barriers to permeation of acetic acid across the interface. We have shown that immiscible films of long-chain organics will have a definite effect on the mass transport across the air–water interface. The transport of volatile species such as water, CO<sub>2</sub>, acetic acid, and other small organics, across the interface of aerosols could have a direct effect on a particle's composition, lifetime, and heterogeneous chemistry. Thus, the properties of an atmospheric aerosol may ultimately be determined by the species that reside at the surface of the particle.

**Acknowledgment.** J.B.G. would like to thank the University of Colorado at Boulder for the Swell fellowship. V.V. acknowledges funding from the NSF.

## References and Notes

- Mayol-Bracero, O. L.; Gabriel, R.; Andreae, M. O.; Kirchstetter, T. W.; Novakov, T.; Ogren, J.; Sheridan, P.; Streets, D. G. *J. Geophys. Res. [Atmos.]* **2002**, *107*, INX2/29/1.
- Allan, J. D.; Alfarra, M. R.; Bower, K. N.; Williams, P. I.; Gallagher, M. W.; Jimenez, J. L.; McDonald, A. G.; Nemitz, E.; Canagaratna, M. R.; Jayne, J. T.; Coe, H.; Worsnop, D. R. *J. Geophys. Res. [Atmos.]* **2003**, *108*, AAC2/1.
- Middlebrook, A. M.; Murphy, D. M.; Thomson, D. S. *J. Geophys. Res. Atmos.* **1998**, *103*, 16475.
- Murphy, D. M.; Thomson, D. S.; Mahoney, T. M. *J. Science* **1998**, *282*, 1664.
- Hamilton, J. F.; Webb, P. J.; Lewis, A. C.; Hopkins, J. R.; Smith, S.; Davy, P. *Atmos. Chem. Phys.* **2004**, *4*, 1279.
- Jacobson, M. C.; Hansson, H. C.; Noone, K. J.; Charlson, R. J. *Rev. Geophys.* **2000**, *38*, 267.
- Rogge, W. F.; Mazurek, M. A.; Hildemann, L. M.; Cass, G. R.; Simoneit, B. R. *Atmos. Environ., Part A: Gen. Topics* **1993**, *27A*, 1309.
- Liu, D.-Y.; Wenzel, R. J.; Prather, K. A. *J. Geophys. Res. [Atmos.]* **2003**, *108*, SOS 14/1.
- Decesari, S.; Facchini, M. C.; Fuzzi, S.; Tagliavini, E. *J. Geophys. Res. Atmos.* **2000**, *105*, 1481.
- Saxena, P.; Hildemann, L. M. *J. Atmos. Chem.* **1996**, *24*, 57.
- Mochida, M.; Kitamori, Y.; Kawamura, K.; Nojiri, Y.; Suzuki, K. *J. Geophys. Res. Atmos.* **2002**, *107*, art. no.
- Barger, W. R.; Garrett, W. D. *J. Geophys. Res.* **1970**, *75*, 4561.
- Tarback, T. L.; Richmond, G. L. *J. Phys. Chem. B* **2005**, *109*, 20868.
- Tervahattu, H.; Juhanoja, J.; Kupiainen, K. *J. Geophys. Res. [Atmos.]* **2002**, *107*, ACH18/1.
- Peterson, R. E.; Tyler, B. *J. Atmos. Environ.* **2002**, *36*, 6041.
- Tervahattu, H.; Juhanoja, J.; Vaida, V.; Tuck, A. F.; Niemi, J. V.; Kupiainen, K.; Kulmala, M.; Vehkamäki, H. *J. Geophys. Res. [Atmos.]* **2005**, *110*, D06207/1.
- Ellison, G. B.; Tuck, A. F.; Vaida, V. *J. Geophys. Res. [Atmos.]* **1999**, *104*, 11633.
- Gill, P. S.; Graedel, T. E.; Weschler, C. J. *Rev. Geophys. Space Phys.* **1983**, *21*, 903.
- Donaldson, D. J.; Vaida, V. *Chem. Rev.* **2006**, *106*, 1445.
- Barnes, G. T. *Colloids Surf., A: Physicochem. Eng. Asp.* **1997**, *126*, 149.
- Langmuir, I.; Langmuir, D. B. *J. Phys. Chem.* **1927**, *31*, 1719.
- Barnes, G. T.; Elliot, A. J.; Grigg, E. C. M. *J. Colloid Interface Sci.* **1968**, *26*, 230.
- Blank, M.; Roughton, F. J. W. *Trans. Faraday Soc.* **1960**, *56*, 1832.
- Archer, R. J.; LaMer, V. K. *J. Phys. Chem.* **1955**, *59*, 200.
- LaMer, V. K.; Healy, T. W.; Alymore, L. A. G. *J. Colloid Sci.* **1964**, *19*, 673.
- Blank, M. *J. Phys. Chem.* **1962**, *66*, 1911.
- Caskey, J. A.; Michelsen, D. L.; To, Y. P. *J. Colloid Interface Sci.* **1973**, *42*, 62.
- Rosano, H. L.; La Mer, V. K. *J. Phys. Chem.* **1956**, *56*, 348.
- Langmuir, I.; Schaefer, V. J. *J. Franklin Inst.* **1943**, *235*, 119.
- Gilman, J. B.; Tervahattu, H.; Vaida, V. *Atmos. Environ.* **2006**, *NA*, NA.
- Daeumer, B.; Niessner, R.; Klockow, D. *J. Aerosol Sci.* **1992**, *23*, 315.
- Garrett, W. D. *J. Atmos. Sci.* **1971**, *28*, 816.
- Xiong, J. Q.; Zhong, M.; Fang, C.; Chen, L. C.; Lippmann, M. *Environ. Sci. Technol.* **1998**, *32*, 3536.
- McNamee, C. E.; Barnes, G. T.; Gentle, I. R.; Peng, J. B.; Steitz, R.; Probert, R. *J. Colloid Interface Sci.* **1998**, *207*, 258.
- Finlayson-Pitts, B. J.; Pitts Jr., J. N. *Chemistry of the Upper and Lower Atmosphere*; Academic Press: San Diego, CA, 2000.
- Donaldson, D. J.; Anderson, D. *J. Phys. Chem. A* **1999**, *103*, 871.
- Jayne, J. T.; Duan, S. X.; Davidovits, P.; Worsnop, D. R.; Zahniser, M. S.; Kolb, C. E. *J. Phys. Chem.* **1991**, *95*, 6329.
- Zhang, H. Z.; Li, Y. Q.; Davidovits, P.; Williams, L. R.; Jayne, J. T.; Kolb, C. E.; Worsnop, D. R. *J. Phys. Chem. A* **2003**, *107*, 6398.
- Donaldson, D. J.; Mmereki, B. T.; Chaudhuri, S. R.; Handley, S.; Oh, M. *Faraday Discuss. Chem. Soc.* **2005**, *130*, 227.
- Sayer, R. M.; Gatherer, R. D. B.; Reid, J. P. *Phys. Chem. Chem. Phys.* **2003**, *5*, 3740.
- Seaver, M.; Peele, J. R.; Manuccia, T. J.; Rubel, G. O.; Ritchie, G. *J. Phys. Chem.* **1992**, *96*, 6389.
- Khan, I.; Brimblecombe, P. *J. Aerosol Sci.* **1992**, *23*, S897.
- Kuramori, M.; Uchida, N.; Suehiro, K.; Oishi, Y. *Bull. Chem. Soc. Jpn.* **2000**, *73*, 829.
- Harkins, W. D. *The Physical Chemistry of Surface Films*; Reinhold: New York, 1952.
- Jefferson, A.; Eisele, F. L.; Ziemann, P. J.; Weber, R. J.; Marti, J. J.; McMurry, P. H. *J. Geophys. Res. [Atmos.]* **1997**, *102*, 19021.
- Garrett, W. D. *J. Atmos. Sci.* **1971**, *28*, 816.
- Chang, D. P. Y.; Hill, R. C. *Atmos. Environ. (1967–1989)* **1980**, *14*, 803.
- Dobson, C. M.; Ellison, G. B.; Tuck, A. F.; Vaida, V. *Proc. Natl. Acad. Sci. U.S.A.* **2000**, *97*, 11864.
- Donaldson, D. J.; Tuck, A. F.; Vaida, V. *Phys. Chem. Chem. Phys.* **2001**, *3*, 5270.
- Seidl, W. *Atmos. Environ.* **2000**, *34*, 4917.
- Brimblecombe, P.; Latif, M. T. *Environ. Chem.* **2004**, *1*, 11.
- Vaida, V.; Tuck, A. F.; Ellison, G. B. *Phys. Chem. Earth Pt. C–Solar-Terra. Planet. Sci.* **2000**, *25*, 195.
- Barnes, G. T. *Adv. Colloid Interface Sci.* **1986**, *25*, 89.
- Blank, M. *Retardation Evaporation Monolayers, Pap., Symp. N.Y.* **1962**, *75*.
- Sebba, F.; Rideal, E. K. *Trans. Faraday Soc.* **1941**, *37*, 273.
- Blank, M. *J. Phys. Chem.* **1961**, *65*, 1698.
- Torn, R. D.; Nathanson, G. M. *J. Phys. Chem. B* **2002**, *106*, 8064.
- Mmereki, B. T.; Chaudhuri, S. R.; Donaldson, D. J. *J. Phys. Chem. A* **2003**, *107*, 2264.
- Lawrence, J. R.; Glass, S. V.; Park, S.-C.; Nathanson, G. M. *J. Phys. Chem. A* **2005**, *109*, 7458.
- Eisner, H. S.; Quince, B. W.; Slack, C. *Discuss. Faraday Soc.* **1960**, *86*.
- Snead, C. C.; Zung, J. T. *J. Colloid Interface Sci.* **1968**, *27*, 25.
- Toossi, R.; Novakov, T. *Atmos. Environ. (1967–1989)* **1985**, *19*, 127.
- Garrett, W. D. *Pure Appl. Geophys.* **1978**, *116*, 316.
- Hanson, H. C.; Wiedensohler, A.; Rood, M. J.; Covert, D. S. *J. Aerosol Sci.* **1990**, *21*, S241.
- Saxena, P.; Hildemann, L. M.; McMurry, P. H.; Seinfeld, J. H. *J. Geophys. Res. [Atmos.]* **1995**, *100*, 18.
- Thomas, E.; Rudich, Y.; Trakhtenberg, S.; Ussyshkin, R. *J. Geophys. Res. [Atmos.]* **1999**, *104*, 16053.
- Garland, R. M.; Wise, M. E.; Beaver, M. R.; DeWitt, H. L.; Aiken, A. C.; Jimenez, J. L.; Tolbert, M. A. *Atmos. Chem. Phys.* **2005**, *5*, 1951.
- Rubel, G. O.; Gentry, J. W. *Particulate Sci. Technol.* **1985**, *3*, 37.
- Demou, E.; Visram, H.; Donaldson, D. J.; Makar, P. A. *Atmos. Environ.* **2003**, *37*, 3529.
- Gilman, J. B.; Eliason, T. L.; Fast, A.; Vaida, V. *J. Colloid Interface Sci.* **2004**, *280*, 234.
- Eliason, T. L.; Gilman, J. B.; Vaida, V. *Atmos. Environ.* **2004**, *38*, 1367.
- Rubel, G. O. *J. Phys. Chem.* **1987**, *91*, 2103.
- Bikerman, J. J. *Physical Surfaces. (Physical Chemistry, a Series of Monographs, Vol. 20)*, 1970.